Research Paper
Computational Methods for Differential Equations
http://cmde.tabrizu.ac.ir
Vol. *, No. *, *, pp. 1-19
DOI:10.22034/cmde.2025.62400.2747

A New Perspective for Simulations of Equal-Width Wave Equation

Selçuk Kutluay, Nuri Murat Yağmurlu, and Ali Sercan Karakaş*
Department of Mathematics, Faculty of Arts and Sciences, Inonu University, Malatya, Turkey.

Abstract

The fundamental aim of the present article is to numerically solve the non-linear Equal-Width Wave (EW) equation. For this purpose, the nonlinear term appearing in the equation is firstly linearized by Rubin-Graves type approach. After that, to reduce the equation into a solvable discretized linear algebraic equation system which is the essential part of this study, the Crank-Nicolson type approximation and cubic Hermite collocation method are respectively applied to obtain the integration in the temporal and spatial domain directions. To demonstrate how good the offered method generates approximate numerical results, six experimental problems exhibiting different wave profiles known as the motion of single, interacting two and three, the Maxwellian initial, undular bore and colliding soliton waves given with different initial and boundary conditions of the EW equation will be taken into consideration and solved. Since only the first model problem has an exact solution among these solitary waves, to measure error magnitudes used widely mean squared and maximum norms between analytical and approximate solutions are calculated and also compared with those from other existing works available in the literature. Furthermore, the three conservation constants known as mass, moment and energy quantities are also computed and presented throughout the wave simulations with increasing time. In addition, a tabular comparison of the newly computed norms and conservation constants show that the current scheme produces better and compatible solutions than those of the most of the previous works with the same parameters. Apart from those, the stability analysis for this present scheme has been illustrated using the von Neumann method.

Keywords. Equal width wave equation, Cubic hermite collocation method, Solitary waves, Stability analysis, Crank-Nicolson type approximation, Rubin-Graves type linearization.

2010 Mathematics Subject Classification. 65L60, 65N35, 74J35, 65D07.

1. Introduction

Most natural phenomena are generally stated by algebraic, integral or differential equations. Non-linear evolution equations are such a commonly and widely utilized around us in order to explain various phenomena in several areas of sciences, however they are taken for granted. When those types of phenomena are investigated in detail, it is seen that most of the nonlinear phenomena which have a crucial role in mathematics and science are generally expressed by partial differential equations which are non linear (PDEs). Most of the time, it is usually hard and also troublesome to deal with and find exact solutions of initial and/or boundary value problems consisting of PDEs. Actually, scientists agree that there is no such a method, scheme or technique yet, it is necessary to deal with almost every type of those equations in itself and solve it. Because of this reason, numerical solutions are usually preferred instead of their exact ones. Due to this fact, most of the scientists turned their attention to the numerical techniques and methods for finding out approximate solutions of those problems. One of such equations is widely known as EW equation. This equation is usually seen as an another way of defining of Korteweg-de Vries (KdV) equation. The equal width wave equation was firstly proposed by Morrison *et al.* [32] and is utilized as an alternative way of defining KdV equation and presented as follows

$$U_t + UU_x - \mu U_{xxt} = 0, \tag{1.1}$$

Received: 08 July 2024 ; Accepted: 25 June 2025.
∗ Corresponding author. Email: ali_sercan_44@hotmail.com.

in which $\mu > 0$.

There have been several analytical and numerical manuscripts about Eq. (1.1) having solitary like solutions and illustrates an equilibrium condition among nonlinear and dispersive effects arising inheritenly from the physical phenomena. Some studies on analytical solutions of Eq. (1.1) can be found in [1, 6, 29, 34]. Since Eq. (1.1) has analytical solutions for only a limited number of initial and boundary conditions, scientists are often focused on seeking approximate numerical solutions. Some of the studies carried out in this sense are as follows: Yağmurlu and Karakaş [44] have found approximate solutions of the equation using cubic trigonometric collocation finite element method (FEM) by a linearization of Rubin-Graves type. Among others, Haar wavelet method[19], collocation method [7], Petrov-Galerkin method [17], least-squares method [46], radial base functions using pseudo-spectral method [43], linearized implicit finite-difference technique [13], lumped Galerkin technique [12], explicit finite difference schemes [36], multi-quadric quasi-interpolation technique [10] and fully implicit finite difference scheme [20] are used in order to get numerical solutions of the equation. Lakestani [28] has presented a numerical technique based on the finite difference and collocation methods for the solution of Korteweg–de Vries (KdV) equation. Lubo ve Duressa [30] have concerned with the numerical treatment of delay reaction-diffusion with the Dirichlet boundary condition. Lakestani and Dehghan [27] have presented a numerical technique based on the finite difference and collocation methods is presented for the solution of generalized Kuramoto–Sivashinsky (GKS) equation. Nemati Saray *et al.* [42] have proposed a numerical method based on the Crank–Nicolson scheme and the Tau method for solving nonlinear Klein–Gordon equation.

The current scheme to be used in this study is a mixture of the orthogonal collocation method and FEM, where the cubic hermite polynomials have been used as a trial function. Since these polynomials satisfy the continuity conditions for trial functions and their several order derivatives at nodes, they produce solutions with continuous derivatives throughout the domain of the problem.

In the present method, the solution region is firstly split in a various number of elements, and next orthogonal collocation is used in each one of these elements, setting the residue equal to zero at two inner mesh points. Nodal points have a key act during the discretization of the equation with respect to x. For the present method, the roots of orthogonal polynomials such as the second degree Legendre and Chebyshev polynomials are usually taken as collocation points. Arora et al. [5] have used the roots of Legendre polynomials at interior collocation points and illustrated that those polynomials present results having less error than Chebyshev polynomials. In addition, they observed that while Chebyshev polynomials produce better results only at cups, Legendre polynomials produce better solutions over the solution domain as well as at the cups. Recently, Kutluay *et al.* [26] have successfully applied collocation finite element method with cubic Hermite basis functions to generate more precise approximate numerical solutions of the heat conduction problem.

In this work, we will present simulations and approximate numerical solutions of Eq. (1.1) using cubic Hermite B-spline based on collocation technique with the help of Crank-Nicolson type approximation. Truly, the basic idea underlying the collocation technique with various B-splines is generally utilized to achieve approximate solutions of non-linear PDEs. Several scientists have used the collocation method based on several bases like classical B-splines, exponential and radial base functions and trigonometric B-splines. Regarding the article itself and its details, one can refer to the articles [3, 4, 15, 16, 18, 21–25, 31, 33, 45] and the references in it.

The present paper has been divided into 7 sections. Section 1 is an introduction to the Cubic Hermite Collocation Method (CHCM). A short explanation of the EW equation is presented in the second section. Sections 3 and 4 detail the implementation of the proposed scheme. Section 5 is about examining the stability of the numerical scheme. Section 6 is devoted to a tabular comparison of the approximate solutions and simulations found by solving six test problems using the present method. The last section, which is section 7, is dedicated to a brief conclusion with a future work.

2. Implementation of the method

In this article, the following EW equation is considered

$$U_t + UU_x - \mu U_{xxt} = 0, \quad -\infty < x < \infty,$$

having the boundary conditions $U \to 0$ when $x \to \pm\infty$.

2.1. **Discretization in spatial variable direction.** For approximate evaluation of any initial and boundary value problem, as in general, consider that spatial domain is chosen a finite interval as $[a,b] \subset \mathbb{R}$and then is split into N equal length elements at x_j $(j = 1(1)N+1)$ so that $a = x_1 < x_2 < \cdots < x_{j-1} < x_j < x_{j+1} < \cdots < x_N < x_{N+1} = b$ where $h = x_{j+1} - x_j$.

During the numerical computations of the problems, since the above mentioned pyhsical boundary conditions are going to be sought in the finite interval $x \in [a,b]$ in Numerical Examples Section, the suitable conditions at the boundaries are going to be used as

$$\begin{cases} U(a,t) = U(b,t) = 0, \\ U_x(a,t) = U_x(b,t) = 0. \end{cases} \tag{2.1}$$

The cubic hermite base functions H_j $(j = 1(1)N+1)$ are taken as [18]

$$H_{2j-1}(x) = \frac{1}{h^3} \begin{cases} (x - x_{j-1})^2 \left[3h - 2(x - x_{j-1})\right], & x_{j-1} \le x \le x_j, \\ \left[h - (x - x_j)\right]^2 \left[h - 2(x - x_j)\right], & x_j \le x \le x_{j+1}, \\ 0, & otherwise, \end{cases} \tag{2.2}$$

$$H_{2j}(x) = \frac{1}{h^3} \begin{cases} -h(x - x_{j-1})^2 \left[h - (x - x_{j-1})\right], & x_{j-1} \le x \le x_j, \\ h(x - x_j)\left[h + (x - x_j)\right]^2, & x_j \le x \le x_{j+1}, \\ 0, & otherwise. \end{cases} \tag{2.3}$$

An approximation to the exact solution $U(x,t)$ denoted by $U_N(x,t)$ is sought in terms of third degree Hermite basis functions given by Equations (2.2) – (2.3)

$$U(x,t) \approx U_N(x,t) = \sum_{j=1}^{N} a_{j+2k-2}(t)\, H_{ji}(x), \tag{2.4}$$

in which a's are time dependent coefficients to be determined which is essential part of this work, the i's ($i = 1$ and $i = 2$) are inner collocation points x_i and k denotes the element number . If one uses the second order Legendre quadrature points η_{ji} for each subinterval $[x_j, x_{j+1}]$, under this condition the Legendre quadrature nodal points now become

$$\eta_{ji} = \frac{x_{j-1} + x_j}{2} + (-1)^i \frac{h_j}{2\sqrt{3}}, \quad 1 \le i \le 2, \quad 2 \le j \le N+1. \tag{2.5}$$

If the following roots of the shifted Legendre polynomial are used in Eq. (2.5)

$$\xi_1 = \frac{1}{2}\left(1 + \frac{1}{\sqrt{3}}\right), \quad \xi_2 = \frac{1}{2}\left(1 - \frac{1}{\sqrt{3}}\right),$$

one gets

$$\frac{\eta_{j1} - x_j}{h_j} = -\xi_1, \quad \frac{\eta_{j2} - x_j}{h_j} = -\xi_2.$$

However, when one uses Chebyshev polynomials, the following roots

$$\xi_1 = \frac{1}{2}\left(1 + \frac{1}{\sqrt{2}}\right), \quad \xi_2 = \frac{1}{2}\left(1 - \frac{1}{\sqrt{2}}\right),$$

are obtained. In this article, both Legendre and Chebyshev polynomial roots will be utilized for the approximate calculations.

In this method, after discretization, a new coordinate variable ξ is defined in any typical element $[x_j, x_{j+1}]$ such that $\xi = (x - x_j)/h$. Thus, the variable x changes in the range $[x_j, x_{j+1}]$, while the new variable ξ changes in the range of $[0,1]$. Thus using the transformation $x = h\xi + x_j$, the following equations are obtained

$$
\begin{aligned}
&H_1(\xi) = (1-\xi)^2(1+2\xi), \quad H_2(\xi) = (1-\xi)^2 \xi h \\
&H_3(\xi) = \xi^2(3-2\xi), \qquad\quad H_4(\xi) = \xi^2(\xi-1)h,
\end{aligned}
$$

$$
\begin{aligned}
&A_1(\xi) = 6\xi^2 - 6\xi, \quad A_2(\xi) = \left(1 - 4\xi + 3\xi^2\right) h \\
&A_3(\xi) = 6\xi - 6\xi^2, \quad A_4(\xi) = \left(3\xi^2 - 2\xi\right) h
\end{aligned}
$$

$$
\begin{aligned}
&B_1(\xi) = 6(2\xi - 1), \quad B_2(\xi) = 2(3\xi - 2) h \\
&B_3(\xi) = 6(1 - 2\xi), \quad B_4(\xi) = 2(3\xi - 1) h.
\end{aligned}
$$

Therefore, the trial function over the k^{th} element is obtained as

$$
U_N(x,t) = \sum_{j=1}^{N} a_{j+2k-2}(t) H_{ji}(x).
$$

The trial functions with their 1^{st} and 2^{nd} order derivatives at the collocation points in terms of local variable ξ are defined as follows

$$
\begin{aligned}
U_N(\xi,t) &= \sum_{j=1}^{4} a_{j+2k-2}(t) H_j(\xi) \\
&= a_{2k-1} H_1(\xi) + a_{2k} H_2(\xi) + a_{2k+1} H_3(\xi) + a_{2k+2} H_4(\xi)
\end{aligned}
$$

$$
\begin{aligned}
U_N^{'}(\xi,t) &= \frac{1}{h} \sum_{j=1}^{4} a_{j+2k-2}(t) A_j(\xi) \\
&= \frac{1}{h}\left[a_{2k-1} A_1(\xi) + a_{2k} A_2(\xi) + a_{2k+1} A_3(\xi) + a_{2k+2} A_4(\xi)\right]
\end{aligned}
$$

$$
\begin{aligned}
U_N^{''}(\xi,t) &= \frac{1}{h^2} \sum_{j=1}^{4} a_{j+2k-2}(t) B_j(\xi) \\
&= \frac{1}{h^2}\left[a_{2k-1} B_1(\xi) + a_{2k} B_2(\xi) + a_{2k+1} B_3(\xi) + a_{2k+2} B_4(\xi)\right].
\end{aligned}
$$

Here A_i and B_i for $i = 1(1)4$ stand for the 1^{st} and 2^{nd} order derivatives of Hermite basis functions, respectively. If Eqs. (2.2) and (2.3) are utilized at the nodes, one finds the following approximations

$$
\begin{aligned}
&U_i = U_N(\xi_i,t) = a_{2k-1} H_{1i} + a_{2k} H_{2i} + a_{2k+1} H_{3i} + a_{2k+2} H_{4i}, \\
&hU_i' = U_N^{'}(\xi_i,t) = a_{2k-1} A_{1i} + a_{2k} A_{2i} + a_{2k+1} A_{3i} + a_{2k+2} A_{4i}, \\
&h^2 U_i^{''} = U_N^{''}(\xi_i,t) = a_{2k-1} B_{1i} + a_{2k} B_{2i} + a_{2k+1} B_{3i} + a_{2k+2} B_{4i},
\end{aligned}
\tag{2.6}
$$

where $H_{ji} = H_j\ (\xi_i)$, $A_{ji} = A_j\ (\xi_i)$ and $B_{ji} = B_j\ (\xi_i)$ for $i = 1, 2$.

Initially, forward finite difference approximation for temporal integration and then collocation FEM utilizing cubic Hermite B-spline basis functions for spatial integration will be implemented. The implementation of the newly proposed method using Hermite B-spline basis functions are more effective due to their several crucial properties like low storage requirement and less manipulations in computer algorithms.

It is worth to note that both of non-linear and linear algebraic equations systems found utilizing any B-spline basis functions have been usually well-conditioned and let the unknowns quantities be specified quite easily. Furthermore, when obtaining the approximations by B-splines, one mostly doesn't come across numerical instability. Apart from these, the coefficient matrices of the algebraic equation system obtained from Hermite splines are comprised of zero input and at the same time easier to be applied on digital computers.

2.2. **Discretization in time variable direction.** Now we are ready to discretize Eq. (1.1) given by

$$U_t + UU_x - \mu U_{xxt} = 0.$$

To do so, first of all, Crank-Nicolson type approximation is applied to Eq. (1.1) in order to get the following discretized scheme

$$\frac{U^{n+1} - U^n}{\Delta t} + \frac{(UU_x)^n + (UU_x)^{n+1}}{2} - \mu \frac{(U_{xx})^{n+1} - (U_{xx})^n}{\Delta t} = 0. \tag{2.7}$$

Then, linearizing the nonlinear term $(UU_x)^{n+1}$ given in Eq. (2.7) by virtue of the Rubin-Graves type approximation [40]

$$(UU_x)^{n+1} = U_x^{n+1} U^n + U^{n+1} U_x^n - U_x^n U^n, \tag{2.8}$$

and substituting (2.8) into (2.7), one gets the following recursive formula to find next time level unknowns

$$U^{n+1}\left(\frac{1}{\Delta t} + \frac{1}{2} U_x^n\right) + \frac{1}{2} U_x^{n+1} U^n - \frac{\mu}{\Delta t} U_{xx}^{n+1} = \frac{1}{\Delta t} U^n - \frac{\mu}{\Delta t} U_{xx}^n. \tag{2.9}$$

When the cubic Hermite base functions and their derivatives given in Eq. (2.6) are used in Eq. (2.9), the following iterative formula is obtained

$$\begin{aligned}
&\left[a_{2k-1}^{n+1} H_{1i} + a_{2k}^{n+1} H_{2i} + a_{2k+1}^{n+1} H_{3i} + a_{2k+2}^{n+1} H_{4i}\right] \left[\frac{1}{\Delta t} + \frac{a_{2k-1}^n A_{1i} + a_{2k}^n A_{2i} + a_{2k+1}^n A_{3i} + a_{2k+2}^n A_{4i}}{2h}\right] \\
&+ \left[\frac{a_{2k-1}^{n+1} A_{1i} + a_{2k}^{n+1} A_{2i} + a_{2k+1}^{n+1} A_{3i} + a_{2k+2}^{n+1} A_{4i}}{h}\right] \left[\frac{a_{2k-1}^n H_{1i} + a_{2k}^n H_{2i} + a_{2k+1}^n H_{3i} + a_{2k+2}^n H_{4i}}{2}\right] \\
&- \frac{\mu}{\Delta t} \left[\frac{a_{2k-1}^{n+1} B_{1i} + a_{2k}^{n+1} B_{2i} + a_{2k+1}^{n+1} B_{3i} + a_{2k+2}^{n+1} B_{4i}}{h^2}\right] \\
&= \left[\frac{a_{2k-1}^n H_{1i} + a_{2k}^n H_{2i} + a_{2k+1}^n H_{3i} + a_{2k+2}^n H_{4i}}{\Delta t}\right] - \frac{\mu}{\Delta t} \left[\frac{a_{2k-1}^n B_{1i} + a_{2k}^n B_{2i} + a_{2k+1}^n B_{3i} + a_{2k+2}^n B_{4i}}{h^2}\right]
\end{aligned} \tag{2.10}$$

in which T is being the desired final time, $\Delta t = T/M$ and $t_n = n\Delta t$ $(n = 1(1)M)$. From Eq. (2.10), a discretized linear algebraic system of equations is obtained. The newly obtained equations are recursive relationships in nature including element parameters vector $\mathbf{a}^n = (a_1^n, ..., a_{2N+1}^n, a_{2N+2}^n)$ in which $t_n = n\Delta t$, $n = 1(1)M$ till the desired time T. When the boundary conditions given in Eq. (2.1) are used and the parameters a_1^n and a_{2N+1}^n in Eq. (2.10) are eliminated as stated following: Using the left boundary condition $U(x_0, t) = a_1^n H_{11} + a_2^n H_{21} + a_3^n H_{31} + a_4^n H_{41} = 0$, since $H_{11} \neq 0$ and $H_{21} = H_{31} = H_{41} = 0$, the condition $a_1^n = 0$ is found. In a similar way, using the right boundary condition $U(x_N, t) = a_{2N-1}^n H_{12} + a_{2N}^n H_{22} + a_{2N+1}^n H_{32} + a_{2N+2}^n H_{42} = 0$, since $H_{32} \neq 0$ and $H_{12} = H_{22} = H_{42} = 0$, the condition $a_{2N+1}^n = 0$ is found.

Finally, one gets a new uniquely solvable algebraic equation system as

$$\mathbf{L}\boldsymbol{a}^{n+1} = \boldsymbol{R}\mathbf{a}^n, \tag{2.11}$$

where $\mathbf{L}$ and $\mathbf{R}$ represent diagonal band matrices of order $2N \times 2N$, $\boldsymbol{a}^n$ and $\boldsymbol{a}^{n+1}$ are known and unknown column matrices of order $2N \times 1$, respectively.

The unknown values $\mathbf{a}_i$ $(i = 1(1)2N)$ in Eq. (2.11) are found and the numerical results of EW equation at the next time level are calculated. This iterative procedure is made again and again for $t_n = n\Delta t$ $(n = 1(1)M)$ till the desired time T. To be able to initiate the iteration procedure, the initial vector $\mathbf{a}^0$ having the elements $\mathbf{a}_{i0}$ $(i = 1(1)2N)$ needs to be calculated. This initial vector has been computed with the help of the initial condition.

2.3. **The initial state.** The vector $\mathbf{a}^0$ given at the initial time is found using the initial and also boundary conditions. Thus, the approximate solution $U_N(x,t)$ given by Eq. (2.4) at $t = 0$ is written as

$$U(x,t) \approx U_N(x,t) = \sum_{j=1}^{N} a_{j+2k-2}^0\,(t)\,H_{ji}(x),$$

in which the a_m^0's are coefficients to be calculated. It is required that the initial numerical approximation $U_N(x,0)$ satisfies the conditions

$$\begin{aligned} &U_N(x_i,0) = U(x_i,0), \quad i = 0,1,...,N, \\ &(U_N)_x(a,0) = (U_N)_x(b,0) = 0. \end{aligned}$$

Therefore, the following initial matrix system is obtained

$$\mathbf{W}\mathbf{a}^0 = \mathbf{b}, \tag{2.12}$$

where

$$\mathbf{W} = \begin{bmatrix} H_{21} & H_{31} & H_{41} & & & & & \\ H_{22} & H_{32} & H_{42} & & & & & \\ & H_{11} & H_{21} & H_{31} & H_{41} & & & \\ & H_{12} & H_{22} & H_{32} & H_{42} & & & \\ & & \ddots & \ddots & \ddots & \ddots & & \\ & & & H_{11} & H_{21} & H_{31} & H_{41} & \\ & & & H_{12} & H_{22} & H_{32} & H_{42} & \\ & & & & & H_{11} & H_{21} & H_{41} \\ & & & & & H_{12} & H_{22} & H_{42} \end{bmatrix},$$

$$\mathbf{a}^0 = [a_2 \ a_3 \ a_4 \ldots, a_{2N-1} \ a_{2N} \ a_{2N+2}]^T,$$

and

$$\mathbf{b} = (U(x_{11},0), U(x_{12},0), U(x_{21},0), \ldots, U(x_{N1},0), U(x_{N2},0))^T.$$

Therefore, the initial solution needed to initialize the iterative scheme (2.11) is found from Eq. (2.12). Then, the iterative procedure is continued for consecutive time step until the desired finish time T.

3. Stability analysis

This part of the article is devoted to the stability analysis of the linear numerical scheme (2.10) proposed for EW equation using the von Neumann method. With this purpose in mind, replacing the Fourier mode

$$a_j^n = \xi^n e^{ij\varphi}, \ i = \sqrt{-1}$$

into Eq. (2.10), one obtains

$$\begin{aligned} &\xi^{n+1} e^{i(2j-1)\varphi}\alpha_1 + \xi^{n+1} e^{i(2j)\varphi}\alpha_2 + \xi^{n+1} e^{i(2j+1)\varphi}\alpha_3 + \xi^{n+1} e^{i(2j+2)\varphi}\alpha_4 \\ &\qquad = \xi^n e^{i(2j-1)\varphi}\beta_1 + \xi^n e^{i(2j)\varphi}\beta_2 + \xi^n e^{i(2j+1)\varphi}\beta_3 + \xi^n e^{i(2j+2)\varphi}\beta_4 \end{aligned} \tag{3.1}$$

in which $\varphi = \beta h$, ξ is the amplification multiplication h and β are respectively spatial step size and mode number, and $\alpha' s$ and $\beta' s$ are as follows

$$\alpha_1 = H_{1i}\Big(\frac{1}{\Delta t} + \frac{a^n_{2k-1}A_{1i} + a^n_{2k}A_{2i} + a^n_{2k+1}A_{3i} + a^n_{2k+2}A_{4i}}{2h}\Big) + A_{1i}\Big(\frac{a^n_{2k-1}H_{1i} + a^n_{2k}H_{2i} + a^n_{2k+1}H_{3i} + a^n_{2k+2}H_{4i}}{2h}\Big) - \frac{\mu}{\Delta t}\frac{B_{1i}}{h^2},$$

$$\alpha_2 = H_{2i}\Big(\frac{1}{\Delta t} + \frac{a^n_{2k-1}A_{1i} + a^n_{2k}A_{2i} + a^n_{2k+1}A_{3i} + a^n_{2k+2}A_{4i}}{2h}\Big) + A_{2i}\Big(\frac{a^n_{2k-1}H_{1i} + a^n_{2k}H_{2i} + a^n_{2k+1}H_{3i} + a^n_{2k+2}H_{4i}}{2h}\Big) - \frac{\mu}{\Delta t}\frac{B_{2i}}{h^2},$$

$$\alpha_3 = H_{3i}\Big(\frac{1}{\Delta t} + \frac{a^n_{2k-1}A_{1i} + a^n_{2k}A_{2i} + a^n_{2k+1}A_{3i} + a^n_{2k+2}A_{4i}}{2h}\Big) + A_{3i}\Big(\frac{a^n_{2k-1}H_{1i} + a^n_{2k}H_{2i} + a^n_{2k+1}H_{3i} + a^n_{2k+2}H_{4i}}{2h}\Big) - \frac{\mu}{\Delta t}\frac{B_{3i}}{h^2},$$

$$\alpha_4 = H_{4i}\Big(\frac{1}{\Delta t} + \frac{a^n_{2k-1}A_{1i} + a^n_{2k}A_{2i} + a^n_{2k+1}A_{3i} + a^n_{2k+2}A_{4i}}{2h}\Big) + A_{4i}\Big(\frac{a^n_{2k-1}H_{1i} + a^n_{2k}H_{2i} + a^n_{2k+1}H_{3i} + a^n_{2k+2}H_{4i}}{2h}\Big) - \frac{\mu}{\Delta t}\frac{B_{4i}}{h^2},$$

$$\beta_1 = \frac{H_{1i}}{\Delta t} - \frac{\mu}{\Delta t}\frac{B_{1i}}{h^2}, \qquad \beta_2 = \frac{H_{2i}}{\Delta t} - \frac{\mu}{\Delta t}\frac{B_{2i}}{h^2}, \qquad \beta_3 = \frac{H_{3i}}{\Delta t} - \frac{\mu}{\Delta t}\frac{B_{3i}}{h^2}, \qquad \beta_4 = \frac{H_{4i}}{\Delta t} - \frac{\mu}{\Delta t}\frac{B_{4i}}{h^2}.$$

Making the required algebraic manipulations in Eq.(3.1), one obtains

$$\xi = \frac{P - iQ}{R + iS}, \tag{3.2}$$

where

$$P = \beta_4\cos 2\varphi + (\beta_1+\beta_3)\cos\varphi + \beta_2, \quad Q = -i(-\beta_4\sin 2\varphi + (\beta_1-\beta_3)\sin\varphi),$$
$$R = \alpha_4\cos 2\varphi + (\alpha_3+\alpha_1)\cos\varphi + \alpha_2, \quad S = i(\alpha_4\sin 2\varphi + (\alpha_3-\alpha_1)\sin\varphi).$$

When one takes the modulus of Eq. (3.2), the inequality $|\xi| \le 1$ is found, and this is the expected requirement for the numerical scheme to be unconditionally stable.

4. Numerical experiments and results

In this section, six widely used experimental problems for the EW equation will be solved for controlling the numerical simulations and the newly found solutions will be compared to those of existing in the literature. All computations are carried out by MATLAB-R2011a on Intel(R) Core(TM) i7-8565U CPU @ 1.80GHz 1.99 GHz machine having 4 GB memory. Since only single solitary wave has an exact solution among the problems considered in the study, the following L_2 and L_∞ quantities called respectively the mean and maximum norm will be calculated to measure the accuracy and reliability of the current numerical scheme

$$L_2 = \left(h\sum_{j=1}^{N+1}|U(x_j,T) - U_N(x_j,T)|^2\right)^{1/2}, \qquad L_\infty = \max_{1\le j\le N+1}|U(x_j,T) - U_N(x_j,T)|.$$

In addition to these error norms, three invariants in the discrete points, of which formulae are given as below [35], are computed

$$I_1 = \int_{-\infty}^{\infty} U\,dx, \quad I_2 = \int_{-\infty}^{\infty}\left(U^2 + \mu U_x^2\right)dx, \quad I_3 = \int_{-\infty}^{\infty} U^3\,dx.$$

Table 1. Comparison of the calculated invariants and error norms of Problem 1 for $h = 0.03$ and $k = 0.05$ ($\mu = 1$, $3c = 0.3$, $x_0 = 10$, $0 \leq x \leq 30$, $0 \leq t \leq 80$).

Method	t	I_1	I_2	I_3	$L_2 \times 10^3$	$L_\infty \times 10^3$
CHCM-L	0	1.1999445724	0.2880000252	0.0576000000	0.000679	0.003911
	10	1.2000134450	0.2880000287	0.0576000016	0.023823	0.032148
	20	1.2000387691	0.2880000300	0.0576000018	0.032656	0.044079
	30	1.2000480346	0.2880000307	0.0576000018	0.035919	0.048468
	40	1.2000512988	0.2880000310	0.0576000018	0.037137	0.050083
	50	1.2000521015	0.2880000310	0.0576000018	0.037608	0.050678
	60	1.2000513090	0.2880000310	0.0576000018	0.037814	0.050897
	70	1.2000480555	0.2880000310	0.0576000018	0.037960	0.050978
	80	1.2000388017	0.2880000310	0.0576000018	0.038334	0.051008
CHCM-C	80	1.2000388189	0.2880000287	0.0576000011	0.040416	0.051117
[44]	80	1.1999851019	0.2879999949	0.0575999982	0.024562	0.009604
[46]	80	1.1964	0.2858	0.0569	7.444	4.373
[17]	80	1.1910	0.28550	0.05582	3.849	2.646
[13]	80	1.20004	0.28799	0.0576	0.125	0.073
[12]	80	1.19995	0.28798	0.05759	0.029	0.021
[8]	80	1.19998	0.28798	0.05759	0.056	0.053
[11]	80	1.23387	0.29915	0.06097	24.697	16.425
[39]	80	1.20004	0.2880	0.0576	0.03882	0.05151
[14]	80	1.20004	0.2880	0.0576	0.03962	0.05446
Analytical		1.2	0.288	0.0576		

All numerical computations are made by using both Cubic Hermite Collocation Method with Chebyshev roots (CHCM-C) and Cubic Hermite Collocation Method with Legendre roots (CHCM-L).

4.1. **Single solitary wave.** The initial experimental problem is widely known as single solitary wave and it has got an exact solution as [32]

$$U(x,t) = 3c \operatorname{sech}^2 \left[k \left(x - x_0 - vt\right)\right], \tag{4.1}$$

in which $k = 1/\sqrt{4\mu}$ is the the solitary wave width, $v = c, \mu = 1$, stands for the wave velocity and $3c$ is taken as the wave amplitude.

Using the solution domain of the problem as $(x,t) \in [a,b] \times [0,T]$, the initial condition is taken from Eq. (4.1) at time $t = 0$ of the following form

$$U(x,0) = 3c \operatorname{sech}^2 \left[k \left(x - x_0\right)\right],$$

and the boundary conditions are given by Eq. (2.1).

The exact solutions of the those invariants are found as follows [17]

$$I_1 = 6\frac{c}{k}, \quad I_2 = 12\frac{c^2}{k} + \frac{48}{5}kc^2\mu, \quad I_3 = \frac{144}{5}\frac{c^3}{k}.$$

The graphics of the simulations of single solitary wave for different values of velocity and amplitudes are plotted in Figure 1. One can easily see from Figure 1 that the amplitudes, velocities and also the shapes of the wave are precisely conserved throughout the simulation. Furthermore, in Table 1, one can see the comparison of our results with some of those existing in the literature. From the table, it is easily seen that the obtained results are better than the other ones except those in Ref. [12]. Table 2 illustrates a comparison of the 3 conservation constants and the error norms of Problem 1 for $h = k = 0.05$ ($\mu = 1$, $3c = 0.03$, $x_0 = 10$, $0 \leq x \leq 30$, $0 \leq t \leq 80$) with their analytical values and those in Refs. [12] and [11]. Again Table 3 puts forward a brief comparison of the 3 conservation constants and the error norms of Problem 1 for values of $h = 0.03$ and $k = 0.2$ ($3c = 0.3$, $\mu = 1$, $x_0 = 10$, $0 \leq x \leq 30$, $0 \leq t \leq 40$) with their analytical values and those in Refs. [46], [38].

Table 4 shows a comparison of the 3 invariants and also the error norms of Problem 1 for several values of N and t at $k = 40$ ($\mu = 1$, $3c = 0.9$, $x_0 = 40$, $0 \leq x \leq 100$). One can clearly see from Table 4 that those results found by taking the shifted roots of the Legendre polynomial as interior collocation points required in the proposed method are much better than those obtained by taking the shifted roots of the Chebyshev polynomial. Since it is known that Legendre polynomials minimize the error and give appropriate results, such results were expected beforehand. Finally, Table 5

Table 2. Comparison of the calculated invariants and error norms of Problem 1 for $h = k = 0.05$ ($\mu = 1$, $3c = 0.03$, $x_0 = 10$, $0 \le x \le 30$, $0 \le t \le 80$).

Method	t	I_1	I_2	I_3	$L_2 \times 10^3$	$L_\infty \times 10^3$
CHCM-L	0	0.1199943936	0.0028800002	0.0000576000	0.000088	0.000391
	10	0.1199954305	0.0028800002	0.0000576000	0.000339	0.000444
	20	0.1199963688	0.0028800002	0.0000576000	0.000657	0.000865
	30	0.1199972178	0.0028800002	0.0000576000	0.000948	0.001249
	40	0.1199979861	0.0028800002	0.0000576000	0.001212	0.001597
	50	0.1199986812	0.0028800002	0.0000576000	0.001451	0.001911
	60	0.1199993102	0.0028800002	0.0000576000	0.001668	0.002196
	70	0.1199998793	0.0028800002	0.0000576000	0.001864	0.002453
	80	0.1200003943	0.0028800002	0.0000576000	0.002041	0.002686
CHCM-C	80	0.1200003983	0.0028800002	0.0000576000	0.002130	0.002697
[12]	80	0.12000	0.00288	0.000058	0.003	0.002
[11]	80	0.12088	0.00291	0.000059	0.330	0.206
Analytical		0.1200	0.00288	0.00006		

Table 3. Comparison of the calculated invariants and error norms of Problem 1 for $h = 0.03$ and $k = 0.2$ ($\mu = 1$, $3c = 0.3$, $x_0 = 10$, $0 \le x \le 30$, $0 \le t \le 40$).

Method	t	I_1	I_2	I_3	$L_2 \times 10^3$	$L_\infty \times 10^3$
CHCM-L	0	1.1999445724	0.2880000252	0.0576000000	0.000679	0.003911
	5	1.1999874409	0.2880000274	0.0576000012	0.000679	0.019904
	10	1.2000134431	0.2880000287	0.0576000016	0.025071	0.032148
	20	1.2000387673	0.2880000301	0.0576000018	0.036187	0.044079
	40	1.2000512978	0.2880000311	0.0576000019	0.048631	0.050084
CHCM-C	40	1.2000513180	0.2880000297	0.0576000015	0.052210	0.050194
[46]	40	1.1967	0.2860	0.0570	3.475	2.136
[38]	40	1.199992	0.2921585	0.05759999	0.07954512	–
Analytical		1.2	0.288	0.0576		

Table 4. Comparison of the calculated invariants and error norms of Problem 1 for various values of N and k at $t = 40$ ($\mu = 1$, $3c = 0.9$, $x_0 = 40$, $0 \le x \le 100$).

Method	(N, k)	I_1	I_2	I_3	L_2	L_∞
CHCM-L						
	$(400, 0.2)$	3.5999999590	2.5920297204	1.5552059235	0.002671	0.001425
	$(400, 0.1)$	3.5999999590	2.5920296695	1.5552058615	0.000696	0.000370
	$(400, 0.05)$	3.5999999590	2.5920296718	1.5552058581	0.000202	0.000107
	$(400, 0.025)$	3.5999999589	2.5920296733	1.5552058580	0.000079	0.000043
	$(200, 0.1)$	3.5999974428	2.5924441834	1.5552857179	0.001251	0.000675
	$(800, 0.1)$	3.5999999994	2.5920018908	1.5552003783	0.000661	0.000354
	$(1600, 0.1)$	3.6000000000	2.5920001237	1.5552000278	0.000659	0.000353
CHCM-C						
	$(400, 0.2)$	3.5998868279	2.5918782898	1.5550774465	0.004919	0.002894
	$(400, 0.1)$	3.5998866685	2.5918790458	1.5550779337	0.003078	0.001896
	$(400, 0.05)$	3.5998866286	2.5918792500	1.5550780676	0.002647	0.001646
	$(400, 0.025)$	3.5998866187	2.5918793020	1.5550781018	0.002542	0.001584
	$(200, 0.1)$	3.5982884438	2.5901738078	1.553355029	0.011636	0.007023
	$(800, 0.1)$	3.5999928133	2.5919922760	1.5551922231	0.001212	0.000717
	$(1600, 0.1)$	3.5999995492	2.5919995049	1.5551995049	0.000788	0.000433
[36]						
	$(400, 0.2)$ EXE	3.600000	2.882298	1.828214	0.0133293	–
	$(400, 0.1)$ EXE	3.599999	2.724104	1.681432	0.00490421	–
	$(400, 0.05)$ EXE	3.600000	2.652641	1.616028	0.00247959	–
	$(400, 0.025)$ E	3.600000	2.652160	1.615533	0.00310718	–
	$(200, 0.1)$ EXE	3.600000	2.837960	1.807345	0.0105221	–
	$(800, 0.1)$ E	3.600000	2.893544	1.833380	0.0163510	–
	$(1600, 0.1)$ E	3.600000	2.896941	1.835213	0.0173992	–

shows a comparison of the 3 invariants and also the error norms of Problem 1 for various values of N and k at $t = 40$ ($\mu = 1$, $3c = 0.9$, $x_0 = 40$, $0 \le x \le 100$). One can also obviously see from both Tables 4 and 5 as h and k decrease so

TABLE 5. Comparison of the calculated invariants and error norms of Problem 1 for various values of N and k at $t = 40$ ($\mu = 1$, $3c = 0.9$, $x_0 = 40$, $0 \le x \le 100$).

Method	(N, k)	I_1	I_2	I_3	$L_2 \times 10^3$	$L_\infty \times 10^3$
CHCM-L						
	$(400, 0.01)$	3.5999999589	2.5920296738	1.5552058580	0.045036	0.025156
	$(400, 0.005)$	3.5999999590	2.5920296739	1.5552058580	0.040248	0.022653
	$(400, 0.0025)$	3.5999999590	2.5920296739	1.5552058580	0.039056	0.022027
	$(400, 0.00125)$	3.5999999590	2.5920296739	1.5552058580	0.038759	0.021871
	$(800, 0.000625)$	3.5999999994	2.5920018861	1.5552003741	0.002455	0.001389
	$(1600, 0.0003125)$	3.6000000000	2.5920001184	1.5552000235	0.000158	0.000089
CHCM-C						
	$(400, 0.01)$	3.5998866159	2.5918793166	1.5550781115	2.513429	1.566399
	$(400, 0.005)$	3.5998866155	2.5918793187	1.5550781128	2.509307	1.563904
	$(400, 0.0025)$	3.5998866154	2.5918793193	1.5550781132	2.507277	1.563280
	$(400, 0.00125)$	3.5998866154	2.5918793194	1.5550781133	2.508020	1.563124
	$(800, 0.000625)$	3.5999928099	2.5919923510	1.5551922755	0.610566	0.384542
	$(1600, 0.0003125)$	3.5999995490	2.5919995203	1.5551995156	0.151612	0.095748
[36]CE						
	$(400, 0.01)$	3.599999	2.612544	1.579549	1.61169	–
	$(400, 0.005)$	3.600000	2.599007	1.567285	0.795278	–
	$(400, 0.0025)$	3.600000	2.592304	1.561220	0.389948	–
	$(400, 0.00125)$	3.600001	2.588970	1.558205	0.188069	–
	$(800, 0.000625)$	3.599999	2.592064	1.556701	0.0999448	–
	$(1600, 0.0003125)$	3.600000	2.592432	1.555950	0.0503415	–

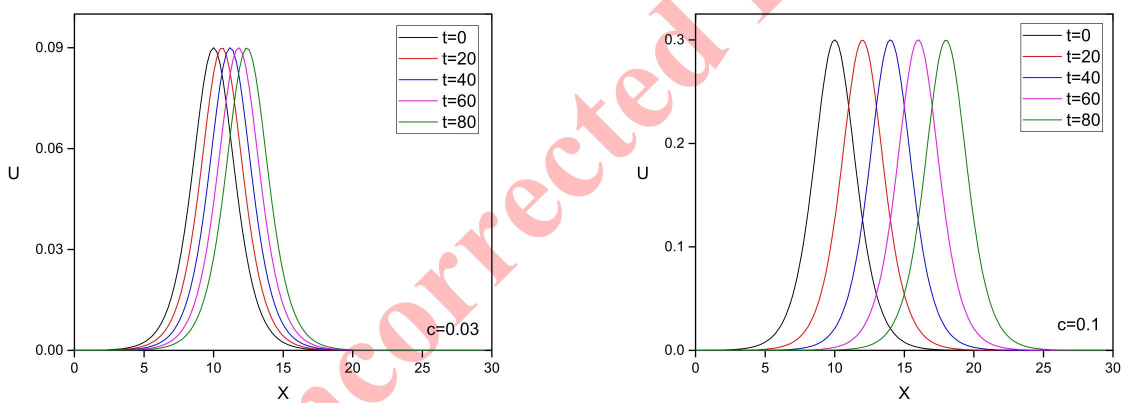

FIGURE 1. Simulations of single solitary wave for velocity values $c = 0.03,\ 0.1$ at $t = 0(20)80$.

the values of the error norms L_2 and L_∞ decrease. In other words, the obtained numerical solution approaches to the analytical solution. This shows that numerical solutions satisfy the expected accuracy.

4.2. **Two solitary waves.** The second test experimental problem has been taken as the interaction of 2 solitary waves. We are going to take into consideration Eq. (1.1) with the solution domain $(x, t) \in [a, b] \times [0, T]$, the usual initial condition [12] and the boundary conditions presented as in Eq. (2.1), respectively

$$U(x, 0) = \sum_{j=1}^{2} 3c_j \sec h^2 \left[0.5 \left(x - x_j - c_j\right)\right],$$

where the parameters $c_1 = 1.5$, $c_2 = 0.75$,$\mu = 1$, $x_1 = 10$, $x_2 = 25$ with $\Delta t = 0.01$ are taken in the region $0 \le x \le 80$. The exact values of the invariants are found as $I_1 = 12 \left(c_1 + c_2\right) = 27$, $I_2 = 28.8 \left(c_1^2 + c_2^2\right) = 81$ and $I_3 = 57.6 \left(c_1^3 + c_2^3\right) = 218.7$.

TABLE 6. Comparison of the calculated invariants of Problem 2 for $h = k = 0.1$ ($\mu = 1$, $c_1 = 1.5$, $c_2 = 0.75$, $x_1 = 10$, $x_2 = 25$, $0 \leq x \leq 80, 0 \leq t \leq 30$).

Method		t	I_1	I_2	I_3
CHCM-L		1	27.000090	81.000450	218.702919
		5	27.000171	81.000368	218.702149
		10	27.000171	80.994156	218.662061
		15	27.000171	80.940889	218.323702
		20	27.000171	80.992358	218.653188
		25	27.000171	81.000154	218.701589
		30	27.000171	81.000478	218.703143
CHCM-C		30	27.000066	80.999907	218.700877
[44]		30	26.999994	81.000511	218.703446
[13]		30	27.00017	80.96848	218.70210
[12]		30	27.00003	81.01719	218.70650
[14]		30	27.00019	81.00045	218.70312
[37]		30	27.12702	80.98988	218.6996
[2]	($h = 0.4$)	30	27.00000	80.999703	218.69966
[41]		30	27.00017	81.00044	218.70304
[9]	($h = 0.4$)	30	27.000582	81.001095	218.726082
[43]	($h = 0.2,\ k = 0.05$)	30	26.93310	80.80028	218.16659
Analytical			27	81	218.7

TABLE 7. Comparison of the calculated invariants of Problem 3 for $h = k = 0.1$ ($\mu = 1$, $c_1 = 4.5$, $c_2 = 1.5$, $c_3 = 0.5$, $x_1 = 10$, $x_2 = 25$, $x_3 = 35$, $0 \leq x \leq 100$, $0 \leq t \leq 15$).

Method		t	I_1	I_2	I_3
CHCM-L		0	77.999971	655.277034	5451.148721
		3	78.000025	651.326045	5384.366499
		6	78.000025	655.118139	5449.115647
		9	78.000025	655.286252	5451.661801
		12	78.000025	655.329978	5451.907342
		15	78.000020	655.337316	5451.947083
CHCM-C		15	77.999656	655.329657	5451.857640
[44]		15	77.999994	655.344625	5452.024410
[37]		15	78.00490	652.3474	5412.232
[2]	($h = 0.4$)	15	77.999984	652.411538	5412.23185
[9]	($h = 0.5$)	15	78.000222	655.341909	5452.481409
[43]	($h = 0.1833,\ k = 0.05$)	15	77.86967	654.09104	5440.78956
[38]		15	77.995390	652.810400	5411.6390
Analytical			78	655.2	5450.4

The collision of 2 solitary waves till time $t = 30$ is presented in Figure 2. One can easily see from this figure that the interaction process started approximately at $t = 10$, and the separation process started approximately at $t = 20$. In the end, 2 waves changed their positions at the initial time. In Table 6, the calculated results have been compared to those existing in the literature. One can obviously see from this table that the newly obtained results are in good harmony with their exact values and also all of the compared ones.

4.3. **Three solitary waves.** The third experimental problem is the collision of 3 solitary waves. Eq. (1.1) will be considered over solution domain $(x, t) \in [a, b] \times [0, T]$, and the boundary conditions (2.1) and the initial condition [43]

$$U(x,0) = \sum_{j=1}^{3} 3c_j \sec h^2 \left[0.5\left(x - x_j - c_j\right)\right],$$

in which the parameters $\mu = 1, c_1 = 4.5$, $c_2 = 1.5$, $c_3 = 0.5$, $x_1 = 10$, $x_2 = 25$, $x_3 = 35$ with $\Delta t = 0.1$ are taken over the region $[0, 100]$. Therefore, the analytical values of the invariants can be found as $I_1 = 12\left(c_1 + c_2 + c_3\right) = 78$, $I_2 = 28.8\left(c_1^2 + c_2^2 + c_3^2\right) = 655.2$ and $I_3 = 57.6\left(c_1^3 + c_2^3 + c_3^3\right) = 5450.4$.

The simulation for the interaction of 3 solitary waves till time $t = 15$ is presented in Figure 3. Furthermore, in Table 7, a comparison of our results with those in the literature is given. One can see from the table that present results are compatibly in good harmony with their exact values and all of the compared ones.

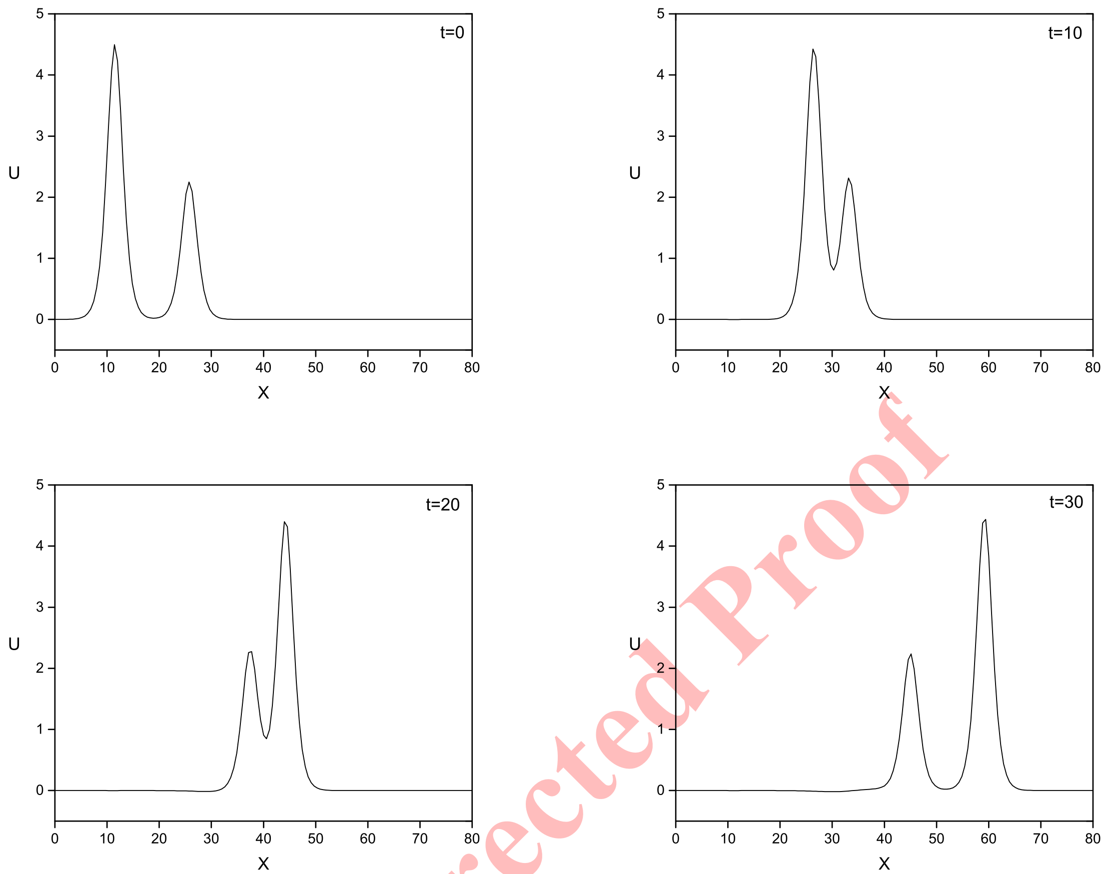

FIGURE 2. The simulation of two solitary waves at times $t = 0$, 10, 20, 30.

4.4. **The Maxwellian initial condition.** The fourth experimental problem dwells on the Maxwellian initial condition of the following form [39]

$$U(x,0) = e^{\left(-(x-20)^2\right)}.$$

The simulations of the Maxwellian pulse are found for constant $\Delta t = 0.01$ and different values of the $\mu = 0.2, 0.04, 0.01$ and 0.001, respectively. Simulation of the waves for the values $\mu = 0.2$, 0.04, 0.01 and 0.001 at $t = 25$ is presented in Figure 4. Moreover, in Table 8, one can see a comparison of the present results with some of those given in the literature. It can be easily seen from the table that the newly obtained results are also in good harmony with the exact values and all of the compared ones.

4.5. **Undular Bore.** In the fifth experimental problem, the EW Equation (1.1) is taken into consideration in the finite range $a \le x \le b$ with the boundary conditions

$$U(a,t) = U_0,$$
$$U(b,t) = 0,$$

and the initial condition

$$U(x,0) = 0.5U_0 \left[1 - \tanh(\frac{x-x_0}{d})\right],$$

to examine undular bore formation. In this equation $U(x, 0)$ stands for the height of the water on the stagnant water at the beginning of simulation, d stands for the slope difference between the deep and stagnant water. The water level change $U(x, 0)$ occurs at the point $x = x_0$. The stagnant water can be observed to the right hand of the zone and at the additional elevation U_0 from the surface $U = 0$ the flow of water moves from the left towards the stagnant water.

In this experimental problem, the conservation constants of I_1, I_2 and I_3 do not remain constant however linearly increase in the following ratios M_1, M_2 and M_3, respectively [17].

$$M_1 = \frac{d}{dt} I_1 = \frac{d}{dt} \int_a^b U dx = \frac{1}{2}(U_0)^2,$$
$$M_2 = \frac{d}{dt} I_2 = \frac{d}{dt} \int_a^b [U^2 + \mu (U_x)^2] dx = \frac{2}{3}(U_0)^3,$$
$$M_3 = \frac{d}{dt} I_3 = \frac{d}{dt} \int_a^b U^3 dx = \frac{3}{4}(U_0)^4.$$

During numerical computations the values $U_0 = 0.1$, $\mu = 0.16666667$ and $x_0 = 0$ are utilized. Therefore, the linearly increasing ratios of the conservation constants for those parameters are found as

$$M_1 = 5e - 3, \ M_2 = 6.66667e - 4, \ M_3 = 7.5e - 5.$$

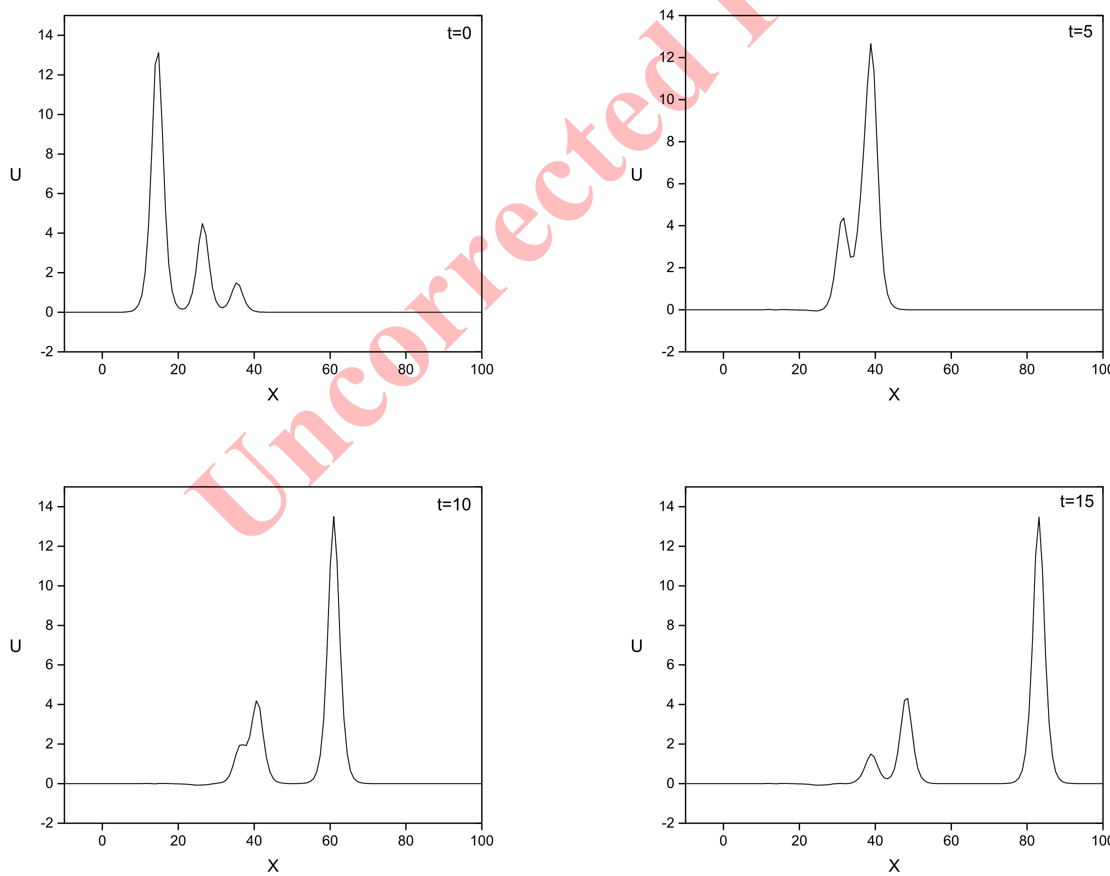

FIGURE 3. The simulation of three solitary waves at times $t = 0, 5, 10, 15$.

Table 8. The computed invariants of Problem 4 and a comparion with those in Refs. [10] and [39] for values of $h = 0.05$ and $k = 0.025$.

		I_1			I_2			I_3		
μ	t	CHCM-L	[10]	[39]	CHCM-L	[10]	[39]	CHCM-L	[10]	[39]
	0	1.77245	1.77245	1.77245	1.37864	1.37864	1.37864	1.02332	1.02333	1.02333
	3	1.77245	1.77245	1.77245	1.37867	1.37867	1.37923	1.02335	1.02336	1.02355
0.1	6	1.77245	1.77245	1.77245	1.37868	1.37868	1.37880	1.02337	1.02337	1.02338
	9	1.77245	1.77245	1.77245	1.37868	1.37869	1.37877	1.02337	1.02338	1.02336
	12	1.77245	1.77245	1.77245	1.37868	1.37869	1.37885	1.02337	1.02338	1.02339
	0	1.77245	1.77245	1.77245	1.31597	1.31598	1.31598	1.02332	1.02333	1.02333
	3	1.77245	1.77245	1.77245	1.31606	1.31606	1.31648	1.02345	1.02345	1.02356
0.05	6	1.77245	1.77245	1.77245	1.31611	1.31611	1.31619	1.02352	1.02352	1.02340
	9	1.77245	1.77245	1.77245	1.31612	1.31611	1.31617	1.02353	1.02353	1.02339
	12	1.77245	1.77245	1.77245	1.31612	1.31611	1.31612	1.02353	1.02353	1.02339
	0	1.77245	1.77245	1.77245	1.28464	1.28464	1.28464	1.02332	1.02333	1.02333
	3	1.77245	1.77238	1.77245	1.28488	1.28487	1.28520	1.02373	1.02372	1.02357
0.025	6	1.77245	1.77254	1.77245	1.28500	1.28499	1.28492	1.02390	1.02392	1.02340
	9	1.77245	1.77233	1.77245	1.28501	1.28496	1.28418	1.02391	1.02386	1.02337
	12	1.77245	1.77253	1.77245	1.28501	1.28497	1.28474	1.02391	1.02390	1.02337
	0	1.77245	1.77245	1.77245	1.26584	1.26585	1.26585	1.02332	1.02333	1.02333
	3	1.77245	1.77247	1.77245	1.26666	1.26572	1.26632	1.02481	1.02293	1.02330
0.01	6	1.77245	1.77253	1.77245	1.26695	1.26579	1.26599	1.02520	1.02297	1.02294
	9	1.77245	1.77252	1.77245	1.26700	1.26562	1.26639	1.02523	1.02295	1.02295
	12	1.77245	1.77253	1.77245	1.26702	1.26566	1.26567	1.02523	1.02292	1.02293

Table 9. Comparison of the computed invariants of Problem 5 for $k = 0.05$ and $h = 0.07$ ($\mu = 0.16666667$, $d = 2$, $x_0 = 0$, $U_0 = 0.1$, $0 \leq t \leq 800$, $-20 \leq x \leq 50$).

Method	t	I_1	I_2	I_3	x	U
CHCM-L	0	1.996500	0.189927	0.018465	−20.00	0.10000
	100	2.496499	0.256594	0.025965	3.73	0.15730
	200	2.996499	0.323261	0.033465	9.40	0.17606
	300	3.496499	0.389928	0.040965	15.35	0.18010
	400	3.996499	0.456595	0.048465	21.37	0.18214
	500	4.496499	0.523262	0.055965	27.46	0.18321
	600	4.996499	0.589929	0.063465	33.55	0.18378
	700	5.496499	0.656596	0.070965	39.71	0.18440
	800	5.996475	0.723263	0.078465	45.87	0.18474
CHCM-C	800	5.995270	0.722959	0.078422	45.87	0.18467
[44]	800	6.003322	0.723860	0.078533	45.87	0.18451
[17]	800	5.994366	0.712677	0.076876	45.70	0.183918
[13]	800	5.996473	0.722126	0.078465	45.87	0.184431
[12]	800	6.003478	0.723605	0.078426	45.87	0.184518
[8]	800	6.003194	0.723867	0.078534	45.85	0.18460
[11]	800	5.669824	0.660997	0.070677	46.73	0.197568
[41]	800	6.002474	0.723860	0.078525	45.85	0.18471

The simulation process for the undular bore at different times t and $d = 2$ is presented in Figure 5. Furthermore, in Table 9, the present results have been compared to some of those available in the literature. One can easily see in this table that the presented method produces good results and they are also are in very good harmony with both their exact values and all of the compared ones.

4.6. **Soliton collision.** As the last example, the interaction of two solitary waves with the initial condition [43]

$$U(x,0) = \sum_{j=1}^{2} 3c_j \sec h^2 \left[\frac{1}{2}(x - x_j - c_j)\right].$$

will be considered.

These solitary waves are also presented like in the phenomena of interaction of 2 solitary waves except the fact that their signs are different and move toward to one another. At collision time, a singularity happens and leaves smaller

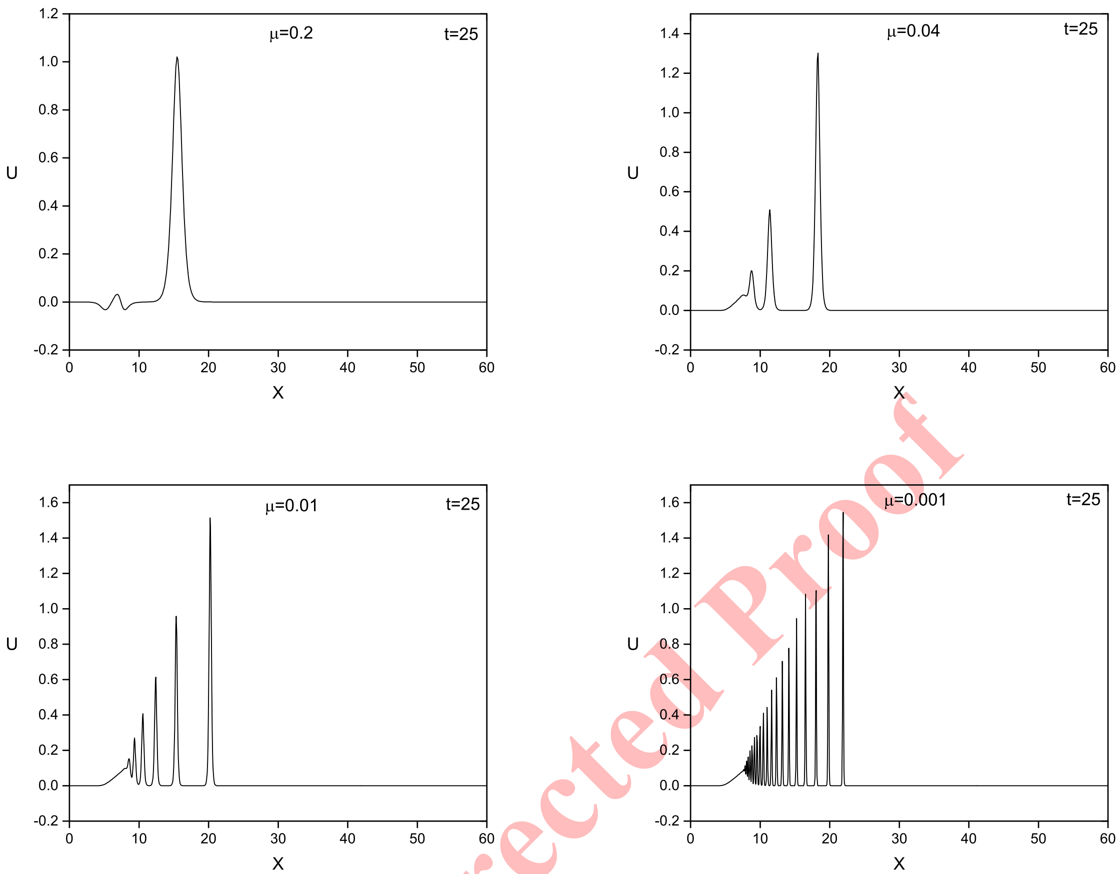

FIGURE 4. The simulations for Maxwellian initial condition for $\Delta t = 0.01$.

waves behind However, when time elapses, these small singularities die out. For the sake of computational aims, the following parameters $c_1 = -1.2$, $c_2 = 1.2$, $\mu = 1$, $x_1 = -20$, $x_2 = 20$ with $\Delta t = 0.1$ are used over the solution domain $[-40, 40]$. The simulation process for the collision of solitons for different values of $t = 0, 15, 50, 100$ is illustrated in Figure 6. One can see from this figure that the waves display the expected physical behavior of the problem.

5. Conclusion

The numerical solutions of the EW equation, which is an alternative to the well-known KdV equation are found using cubic Hermite B-spline collocation FEM. To be able to establish the efficiency and accuracy of the presented method with the help of the Crank-Nicolson type approximation its validity, six test problems are considered and the obtained results are tested by comparing with the previously published ones especially using the error norms L_2 and L_∞. It can be seen from all the computed results that the presented numerical scheme produces reasonable accurate results which are also in good agreement with exact ones and at the same time those of other researchers for the same parameters. About possible future studies, the currently presented method may also easily and successfully be used to find the numerical solutions of other frequently used non-linear PDEs seen in various branches of mathematics and science that have a crucial role in modelling natural phenomena.

Author contributions. All of the authors certify that they contributed sufficiently in the present study to take public responsibility about the content, which includes participation in the planning, analysis, design, and implementation

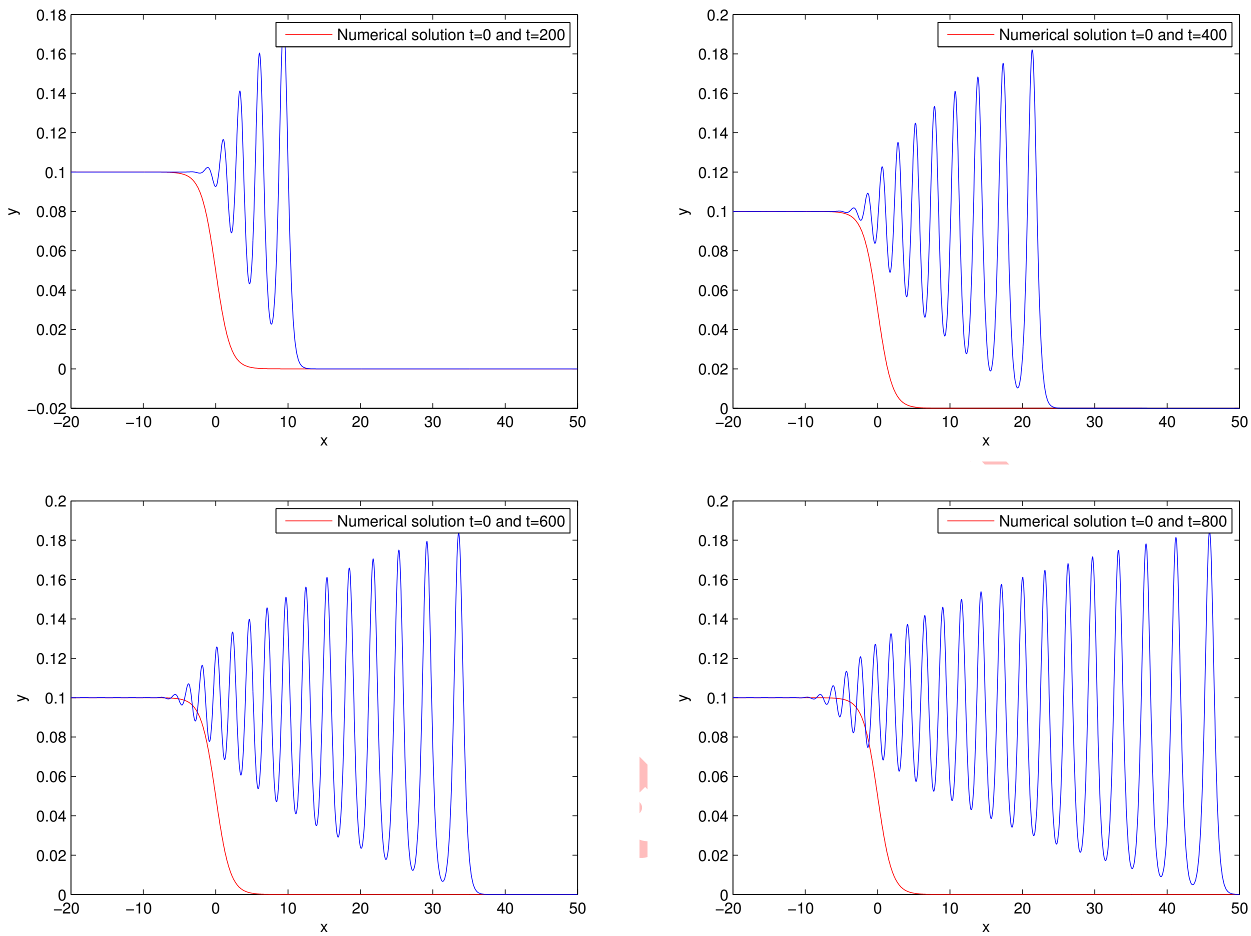

FIGURE 5. The profiles and undulation profiles for $d = 2$ at different times.

of the manuscript. Moreover, each author guarantees that the presented material or similar one has not been and is not going to be submitted to or published in any other journal.

Financial disclosure. One of the authors, Ali Sercan Karakaş, is funded by 2211-A National PhD Scholarship Program, The Scientific and Technological Research Council of Türkiye.

Conflict of interest. We, the authors, declare that there is no conflict of interests regarding the publication of this article.

5.1. **Data availability.** Data will be made available on acceptable request.

5.2. **Declaration of Ethical Standards.** The authors of the present manuscript clearly declare that all of the methods and schemes used in the manuscript do not need any ethical committee and/or legal special requirement or permission.

The authors also declare that this manuscript has been orally presented in abstract form in "The 8th International Conference on Computational Mathematics and Engineering Sciences / 17-19 May. 2024, Şanlıurfa – Türkiye."

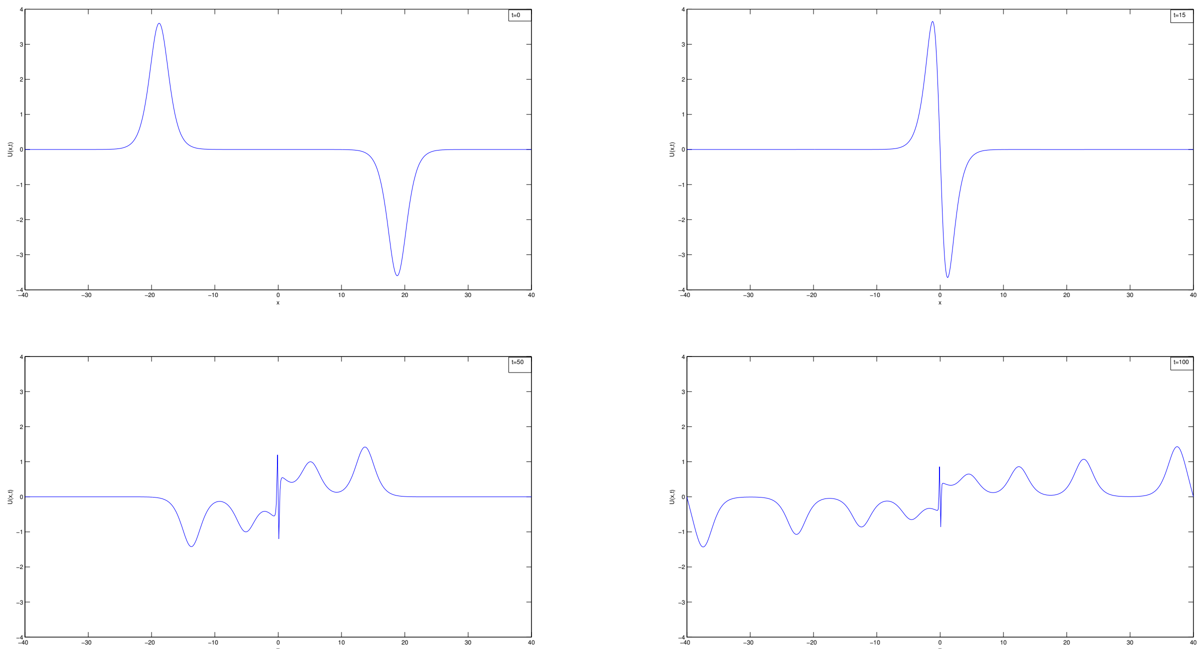

FIGURE 6. Clash of two solitary waves.

References

[1] H. A. Ali, A Biswas, and K. R. Raslan, *Application of He's Exp-function method and semi-inverse variational principle to equal width wave (EW) and modified equal width wave (MEW)*, Int. J. Phy. Sci., *7*(7) (2012), 1035–1043.

[2] A. H. A. Ali, *Spectral method for solving the equal width equation based on Chebyshev polynomials*, Nonlinear Dyn. *51* (2008), 59–70.

[3] S. Arora, R. Jain, and V. K. Kukreja, *Solution of Benjamin-Bona-Mahony-Burgers equation using collocation method with quintic Hermite splines*, Appl. Math. Comput., *154* (2020), 1–16.

[4] S. Arora and I. Kaur, *Applications of Quintic Hermite collocation with time discretization to singularly perturbed problems*, Appl. Math. Comput., *316* (2018), 409–421.

[5] S. Arora, S. S. Dhaliwal, and V. K. Kukreja, *Computationally efficient technique for weight functions and effect of orthogonal polynomials on the average*, Appl. Math. Comput., *186* (2007), 623–631.

[6] J. Biazar and Z. Ayati, *Application of the Exp-function method to the equal-width wave equation*, Phys. Scr., *78* (2008), 045005 (4pp).

[7] I. Dağ and O. Ersoy, *The exponential cubic B-spline algorithm for equal width equation*, Adv. Studies Contemp. Math., *25*(4) (2015), 525–535.

[8] İ. Dağ and B. Saka, *A cubic B-spline collocatıon method for the EW equatıon*,Math. Comput. Appl., *9*(3) (2004), 381–392.

[9] Y. Dereli and R. Schaback, *The Meshless Kernel-Based Method of Lines for solving the Equal Width Equation,* Appl. Math. Comput., *219* (2013), 5224–5232.

[10] S. Dhawan, T. Ak, and G. Apaydın, *Algorithms for numerical solution of the equal width wave equation using multi-quadric quasi-interpolation method*, Int. J. Mod. Phys. C, *30* (2019).

[11] A. Dogan, *Application of Galarkin's method to equal width wave equation*, Appl. Math. Comput., *160* (2005), 65–76.

[12] A. Esen, *A numerical solution of the equal width wave equation by a lumped Galarkin method*, Appl. Math. Comput., *168* (2005), 270–282.

[13] A. Esen and S. Kutluay, *A linearized implicit finite-difference method for solving the equal width wave equation*, Int. J. Comput. Math., *83*(3) (2006), 319–330.

[14] H. Fazal-i, A. Inayet and A. Shakeel, *Septic B-spline Collocation method for numerical solution of the Equal Width Wave (EW) equation*, Life Science Journal, *10* (2013), 253–260.

[15] I. A. Ganaie, S. Arora, and V.K. Kukreja, *Cubic Hermite collocation solution of Kuramoto–Sivashinsky equation*, Int. J. Comput. Math., *93*(1) (2016), 223–235.

[16] I. A. Ganaie, B. Gupta, N. Parumasur, P. Singh, and V. K. Kukreja, *Asymptotic convergence of cubic Hermite collocation method for parabolic partial differential equation*, Appl. Math. Comput., *220* (2013), 560–567.

[17] L. R. T. Gardner, G. A. Gardner, F. A. Ayoup, and N. K. Amein, *Simulations of the EW undular bore,* Commun. Numer. Methods Eng., *13* (1997), 583–592.

[18] I. A. Ganaie and V. K. Kukreja, *Numerical solution of Burgers' equation by cubic Hermite collocation method*, Appl. Math. Comput., *237* (2014) 571–581.

[19] A. Ghafoor and S. Haq, *An efficient numerical scheme for the study of equal width equation*, Results Phys., *9* (2018), 1411-1416.

[20] B İnan and A. R. Bahadır, *A numerical solution of the equal width wave equation using a fully implicit finite difference method*, Turkish J. Math. and Comp. Sci., (2014), Article ID 20140037, 1-14.

[21] S. P. Kaur, A. K. Mittal, V. K. Kukreja, A. Kaundal, N. Parumasur, and P. Singh, *Analysis of a linear and non-linear model for diffusion–dispersion phenomena of pulp washing by using quintic Hermite interpolation polynomials*, Afrika Matematika, *32* (2021), 997-1019.

[22] S. P. Kaur, A. K. Mittal, V.K. Kukreja, N. Parumasur, and P. Singh, *An efficient technique for solution of linear and nonlinear diffusion-dispersion models*, AIP Conference Proceedings, 2018.

[23] N. A. Kudryashov, *Generalized Hermite polynomials for the Burgers hierarchy and point vortices*, Chaos, Solitons Fractals, *151* (2021), 111256.

[24] A. Kumari and V. K. Kukreja, *Robust septic Hermite collocation technique for singularly perturbed generalized Hodgkin–Huxley equation*, Int. J. Comput. Math., 2021.

[25] A. Kumari and V. K. Kukreja, *Septic Hermite collocation method for the numerical solution of Benjamin–Bona–Mahony–Burgers equation*, J. Differ. Equations Appl., *27* (2021), 1193–1217.

[26] S. Kutluay, N. M. Yağmurlu, and A. S. Karakaş, *An Effective Numerical Approach Based on Cubic Hermite B-spline Collocation Method for Solving the 1D Heat Conduction Equation*, New Trends in Math. Sci., *10*(4) (2022), 20–31.

[27] M. Lakestani and M. Dehghan, *Numerical solutions of the generalized Kuramoto–Sivashinsky equation using B-spline functions*, Appl. Math. Modell. , *36*(2) (2012), 605–617.

[28] M. Lakestani, *Numerical solutions of the KdV equation using B-spline functions*, ran. J. Sci. Technol. Trans. Electr. Eng., Transactions A: Science, *41* (2017), 409–417.

[29] D. Lu, A. R. Seadawy, and A. Ali, *Dispersive traveling wave solutions of the Equal-Width and Modified Equal-Width equations via mathematical methods and its applications*, Results Phys., *9* (2018), 313–320.

[30] G. T. Lubo and G. F. Duressa, *Linear B-spline finite element Method for solving delay reaction diffusion equation* Comput. Methods Differ. Equ., *11*(1) (2023), 161–174.

[31] A. K. Mittal, I. A. Ganaie, V. K. Kukreja, N. Parumasur, and P. Singh, *Solution of diffusion–dispersion models using a computationally efficient technique of orthogonal collocation on finite elements with cubic Hermite as basis*, Comp. and Chem. Eng., *58* (2013), 203–210.

[32] P. J. Morrison, J. D. Meiss, and J. R. Cary, *Scattering of Regularized-Long-Wave solitary waves*, Physica 11D, (1984), 324–336.

[33] A. H. Msmali, M.Tamsir, and A. A. H. Ahmadini, *Unified and extended trigonometric B-spline DQM for the numerical treatment of three-dimensional wave equations*, Ain Shams Eng. J. , *15*(2) (2024), 102382.

[34] R. I. Nuruddeen, K. S. Aboodh, and K. K. Ali, *Investigating the tangent dispersive solitary wave solutions to the Equal Width and Regularized Long Wave equations*, J. King Saud Univ. Sci..

[35] P. J. Olver, *Euler operators and conservation laws of the BBM equation*, Math Proc. Camb. Phil. Soc. *85* (1979), 143–160.

[36] J. I. Ramos, *Explicit finite difference methods for the EW and RLW equations*, Appl. Math. Comput., *179* (2006), 622–638.

[37] K. R. Raslan, *A computational method for the equal width equation*, Int. J. Comput. Math., *81* (2004), 63–72.

[38] K. R. Raslan, *Collocation method using quartic B-spline for the equal width (EW) equation*, Appl. Math. Comput., *168* (2005), 795–805.

[39] T. Roshan, *A Petrov-Galerkin Method for Equal width equation*, Appl. Math. Comput., *218* (2011), 2730–2739.

[40] S. G. Rubin and R. A. Graves, *A cubic spline approximation for problems in fluid mechanics*, National aeronautics and space administration, Technical Report, Washington, 1975.

[41] B. Saka, I. Dağ, Y. Dereli and A. Korkmaz, *Three different methods for numerical solutions of the EW equation,* Eng. Anal. Boundary Elem., *32* (2008), 556-566.

[42] B. Nemati Saray, M. Lakestani, and C. Cattani, *Evaluation of mixed Crank–Nicolson scheme and Tau method for the solution of Klein–Gordon equation* Appl. Math. Comput., *331* (2018), 169–181.

[43] M. Uddin, *RBF-PS scheme for solving the equal width equation*, Appl. Math. Comput., *222* (2013), 619–631.

[44] N. M. Yağmurlu and A. S. Karakaş, *Numerical solutions of the equal width equation by trigonometric cubic B-spline collocation method based on Rubin–Graves type linearization*, Numer. Methods Partial Differ. Equations, *36* (2020), 1170–1183.

[45] A. Yousaf, T. Abdeljawad, M. Yaseen and M. Abbas, *Novel Cubic Trigonometric B-Spline Approach Based on the Hermite Formula for Solving the Convection-Diffusion Equation*, Math. Problems in Eng., (2020).

[46] S. I. Zaki, *A least-squares finite element scheme for the EW equation,* Comp. Meth. Appl. in Mech. Eng., *189* (2000), 587–594.